EEET ECOLOGICAL ENGINEERING & ENVIRONMENTAL TECHNOLOGY

Ecological Engineering & Environmental Technology, 2026, 27(4), 315–327
https://doi.org/10.12912/27197050/218928
ISSN 2719–7050, License CC-BY 4.0

Received: 2026.02.18
Accepted: 2026.03.16
Published: 2026.04.01

Competitive adsorption of Cu(II), Cd(II), and Ni(II) on acacia-derived fibrous carbon: Selectivity shift and AICc-based model selection

Lita Darmayanti[1*], David Andrio[1], Elvi Yenie[1], Endang Sri Winih[1]

[1] Department of Environmental Engineering, Universitas Riau, Kampus Bina Widya Simpang Baru, Pekanbaru, 28293, Indonesia
* Corresponding author's e-mail: litadarmayanti@eng.unri.ac.id

ABSTRACT

Heavy metal contamination of aquatic systems poses persistent environmental and public health challenges. However, the mechanisms governing competitive adsorption of multiple metal ions on biomass-derived carbon materials remain insufficiently understood. In this study, fibrous activated carbon was synthesized from Acacia mangium leaf waste via one-step pyrolysis combined with KOH activation. The resulting material exhibited a high specific surface area (~800 m^2/g) and a hierarchical micro-mesoporous structure. Competitive adsorption of Cu(II), Cd(II), and Ni(II) was systematically investigated in single- and multi-metal systems. Kinetic and isotherm models were evaluated using the corrected Akaike information criterion (AICc) to ensure statistically robust model selection. The Elovich model provided the lowest AICc values for all three metals, indicating heterogeneous surface chemisorption. In single-metal systems, adsorption affinity followed the order Cd(II) > Cu(II) > Ni(II), consistent with trends in hydration free energy. In contrast, under competitive conditions, selectivity shifted to Cu(II) > Cd(II) > Ni(II), suggesting that coordination stability plays a more dominant role in multicomponent systems. The results establish that adsorption selectivity on fibrous carbon is not intrinsic to individual ion properties but is dynamically redefined under competitive conditions by coordination stability effects.

Keywords: *Acacia mangium*, fibrous carbon, selectivity shift, competitive adsorption, coordination stability.

INTRODUCTION

Wastewater containing heavy metals (HM) poses a persistent environmental and public health challenge due to their toxicity, persistence, and bioaccumulative nature (Chen et al., 2022; Guo and Yang, 2016; Tan et al., 2015). Industrial effluents frequently contain Cu(II), Ni(II), and Cd(II), which, although some are essential micronutrients at trace levels, become toxic at elevated concentrations (Das and Poater, 2021; Laus and De Favere, 2011). These metals can enter aquatic food webs and drinking water sources, leading to bioaccumulation, bioconcentration, and biomagnification in aquatic organisms and ultimately in humans (Ayach et al., 2024; Bharti, 2024). Therefore, removing HM from wastewater to environmentally safe levels prior to discharge is critically required.

Various physicochemical technologies, including reverse osmosis, electrolysis, ion exchange, chemical precipitation, and adsorption, have been applied to remove HM from contaminated water (Ayach et al., 2024; Ciobanu et al., 2024). While membrane-based and electrochemical methods can achieve high removal efficiencies, their practical implementation is often limited by high operational costs, energy demand, and secondary waste generation. Among available approaches, adsorption has attracted sustained attention due to its operational simplicity, adaptability over a wide concentration range, and compatibility with diverse sorbent materials (Jorge et al., 2024). The development of cost-effective and sustainable adsorbents remains a central challenge for improving the practical feasibility of adsorption-based treatment systems. In this context, agricultural and industrial biomass wastes have

emerged as promising precursors for sorbent production, aligning with circular economy strategies and resource valorization principles (Ferraz and Pyka, 2023; Moustakas and Loizidou, 2024).

The utilization of biomass-derived materials for HM removal has been widely investigated (Liu et al., 2020; Sandoval-Flores et al., 2018; Wang et al., 2023; Wang et al., 2020). Adsorption performance strongly depends on both the physicochemical characteristics of the precursor and the applied synthesis strategy (Karthikeyan et al., 2007; Raji et al., 2023). The presence of surface functional groups, such as amino, carboxyl, hydroxyl, and amide moieties, plays a critical role in metal binding through electrostatic attraction, ion exchange, and surface complexation mechanisms (Kumar et al., 2024; Vieira and Volesky, 2010). Metal uptake by biomass-based sorbents is generally governed by a combination of processes, including ligand–metal complex formation, surface precipitation, and ion exchange interactions (Abbas et al., 2018; Shamim, 2018; Wang et al., 2024). Therefore, tailoring surface chemistry and pore structure is essential for enhancing adsorption efficiency and selectivity.

Lignocellulosic biomass represents an abundant and renewable carbon source for adsorbent production. Waste streams from the pulp and paper industry, particularly those derived from acacia species, offer a consistent and underutilized feedstock. Acacia biomass is characterized by high cellulose (45–50%) and hemicellulose (15–20%) contents with relatively low lignin (9–15%) (Amini et al., 2017), favoring carbonization and pore development during activation. Previous studies have shown that activated carbon derived from acacia leaves can exhibit fibrous morphologies with nanoscale diameters (62–124 nm) (Apriwandi et al., 2020), facilitating ion transport within hierarchical pore networks (Keshavarz et al., 2022). Compared to silica-rich biomass such as rice husk, which often contains >20% ash, acacia biomass offers higher fixed carbon content and lower ash levels (4.5–5.6%), enhancing its suitability as a precursor for activated carbon production (Alam et al., 2020; Kra et al., 2019).

While the adsorption behavior of individual metal ions has been widely characterized, the extent to which selectivity patterns and governing mechanisms persist under competitive multimetal conditions remains insufficiently clarified. Consequently, it remains unresolved whether the selectivity order observed in isolated systems is preserved under competitive conditions or whether interfacial binding mechanisms are fundamentally altered. In addition, kinetic and isotherm model selection is frequently based solely on the coefficient of determination (R^2), which may lead to biased mechanistic interpretation, particularly for nonlinear adsorption models (Pinto et al, 2024; Danat et al., 2026). We hypothesize that (i) competitive adsorption induces a measurable shift in selectivity order compared to single-metal systems, and (ii) the dominant adsorption mechanism transitions from hydration-energy-controlled behavior to coordination-stability-driven interactions under multimetal conditions. Furthermore, we hypothesize that model discrimination based on the corrected Akaike information criterion (AICc) provides more reliable mechanistic interpretation than conventional R^2-based evaluation. The objective of this study is to determine whether competitive interactions among Cu(II), Cd(II), and Ni(II) on acacia-derived fibrous carbon alter adsorption selectivity and governing mechanisms, using statistically rigorous AICc-based model selection to establish a mechanistically grounded interpretation of multimetal adsorption behavior.

MATERIALS AND METHODS

Preparation of fibrous carbon

Acacia leaves were first dried at 150 °C in an oven for 4 h and subsequently ground and sieved through a 60-mesh sieve. The chemical activation was performed by immersing the ground leaves in 0.5 M KOH (Merck) at a 1:5 (g/mL) ratio, followed by stirring at 80 °C and 150 rpm for 2 h. One-stage integrated pyrolysis, combining carbonization and physical activation, was conducted under N_2. Carbonization was performed by heating from ambient temperature to 500 °C at 3 °C/min, and physical activation was carried out in a CO_2 atmosphere at 800 °C for 2 h. The resulting carbon was thoroughly washed with distilled water until a neutral pH was achieved.

Characterization of fibrous carbon

The textural properties of the fibrous carbon were determined using multi-point BET analysis (Quantachrome SA analyzer, QuadraWin ©2000-16) to obtain specific surface area (m^2/g), total

pore volume (cm^3/g), and pore size distribution (nm). Functional groups were analyzed by FTIR spectroscopy using a Shimadzu Prestige 21 spectrometer with KBr pellets in the range 4000–400 1/cm. The surface morphology and fibrous structure were examined via FE-SEM (Thermo Scientific Quattro S) at multiple magnifications.

HM solutions and measurements

Stock solutions of Ni(II), Cd(II), and Cu(II) were prepared by dissolving $NiSO_4 \cdot 6H_2O$, $CdSO_4 \cdot 8H_2O$, and $CuSO_4 \cdot 5H_2O$ (Merck) in distilled water to a concentration of 100 mg/L. For single-metal adsorption experiments, the metal ion concentrations ranged from 20 to 80 mg/L. Binary systems were prepared as Cd(II)–Ni(II), Cu(II)–Ni(II), and Cu(II)–Cd(II), while the ternary system contained Cu(II), Cd(II), and Ni(II). Solutions were diluted from stock to achieve the desired concentrations for adsorption experiments.

Adsorption experiments

Batch adsorption experiments for each metal (Cd(II), Ni (II), and Cu (II)) were carried out at 30 mg/L and pH 5. The solution pH was controlled utilizing 0.1 M NaOH/HCl. This was followed by adding 0.4 g of acacia leaf fibrous carbon to 100 mL of metal solution in a 250 mL Erlenmeyer flask. The Erlenmeyer flask was shaken at 120 rpm for 150 minutes at ambient temperature. After filtering the sample applying WhatmanTM filter paper with a 0.45 μm pore size (PS), the metal concentration was measured using ICP-OES Agilent 5100X. The experiments were conducted in triplicate. The adsorption isotherm experiment was conducted at seven concentrations from 20–80 mg/L. The kinetic study was performed over 5–150 min, applying 0.4 g of adsorbent and 100 ml of metal solution at pH 5 and a 30 mg/L initial concentration.

Adsorption kinetics

To identify the rate-controlling step and the interaction, the kinetic data were fitted to nonlinear forms of the Lagergren PFO (pseudo-first order), PSO (pseudo-second order), and Elovich models. Additionally, the Weber Morris intra-particle diffusion model was employed to evaluate diffusion resistances. The equations are as follows:

$$q_t = q_e\left(1 - e^{-k_1 t}\right) \quad (1)$$

$$q_t = \frac{k_2 q_e^2 t}{1 + k_2 q_e t} \quad (2)$$

$$q_t = \frac{1}{\beta} ln(1 + \alpha\beta t) \quad (3)$$

$$q_t = k_{id} t^{0.5} + C \quad (4)$$

where: qe and qt (mg/g) – total ions at equilibrium and at a specific time (t in min), k_1 – Lagergren PFO rate constant (min^{-1}), k_2 – the PSO rate constant (g/mg.min), α (mg/g.min) – initial adsorption rate, β (g/mg) – the surface heterogeneity constant, k_{id} ($mg/g.min^{0.5}$) – intra particle diffusion rate constant, C (mg/g) – a constant proportional to the boundary layer thickness.

Single, binary, and ternary adsorption equilibrium isotherms

The Langmuir adsorption isotherm model can be employed to forecast single metal, and multimetal adsorption.

$$Langmuir: q_e = \frac{K_L q_m C_e}{1 + K_L C_e} \quad (5)$$

$$Separation\ factor\ (R_L): R_L = \frac{1}{1 + K_L C_0} \quad (6)$$

$$Freundlich: q_e = K_F C_e^{1/n} \quad (7)$$

$$Temkin: q_e = \frac{RT}{b} ln(A_T C_e) \quad (8)$$

To describe multimetal adsorption, the extended Langmuir isotherm model (Berber-Mendoza et al., 2018; Wang and Li, 2009) can be used as follows.

$$q_{e,i} = \frac{K_{L,i} q_{m,i} C_{e,i}}{1 + \sum_{j-1}^{N} K_{L,j} C_{e,j}} \quad (9)$$

where: q_m – maximum adsorption capacity (mg/g), K_L – Langmuir constant (L/mg), K_F – Freundlich constant showing the adsorption capacity $(mg/g)(L/mg)^{1/n}$, n – Freundlich exponent related to adsorption intensity, R – universal gas constant (J/mol.K), T – temperature (K), b – adsorption energy variation (J/mol), A_T – equilibrium binding constant (L/mg).

Data analysis

The percentage of metal removal (R%) was calculated using the following equation:

$$R\% = \frac{C_0 - C_e}{C_o} \times 100\% \quad (10)$$

where: C_o and C_e (mg/L) are the initial and equilibrium concentrations of the metal ion in solution, respectively.

The equilibrium adsorption capacity (q_e, mg/g) of the adsorbent was determined from a mass balance of the batch system:

$$q_e = \frac{(C_0 - C_e)V}{m} \quad (11)$$

where: q_e expresses the adsorbent's equilibrium AC, C_o and C_e show the first and equilibrium concentrations (mg/L), V indicates the solution volume (L), and m demonstrates the adsorbent weight (g).

RESULTS AND DISCUSSION

Characterization of acacia leaf fibrous carbon

Brunauer-Emmett-Teller (BET)

The BET characterization results for acacia fibrous carbon are described in Table 1. SA is a vital factor in obtaining the adsorbent effectiveness. Specifically, an adsorbent larger SA corresponds to greater AC. The SA obtained in this analysis is based on the BET test results was 800.405 m²/g, with a 1.111 nm average PS and a 0.444 cm³/g total pore volume (PV). The adsorption process exhibits a type I and IV adsorption isotherms combination (Figure 1), indicating that fibrous carbon has hierarchical pores consisting of micro-pores (0.039 cm³/g) and mesopores (0.405 cm³/g). The combination of micropores and mesopores is very favorable for HM adsorption processes because micropores provide many binding sites, while mesopores ensure that metal ions can quickly diffuse into the adsorbent structure (Kim et al., 2020). This result exceeded that of the prior study (Darmayanti et al., 2023), indicating that the addition of physical activation time could significantly increase both adsorbent's total PV and SA.

FTIR analysis

FTIR analysis (Figure 2) is applied to pinpoint the functional groups and bonds in acacia fibrous carbon based on the wave numbers obtained.

Table 1. Characterization of the acacia carbon nanofiber with the BET

SA	PV	Average PS	Micro volume	Meso volume
800.405 m²/g	0.444 cm³/g	1.111 nm	0.039 cm³/g	0.405 cm³/g

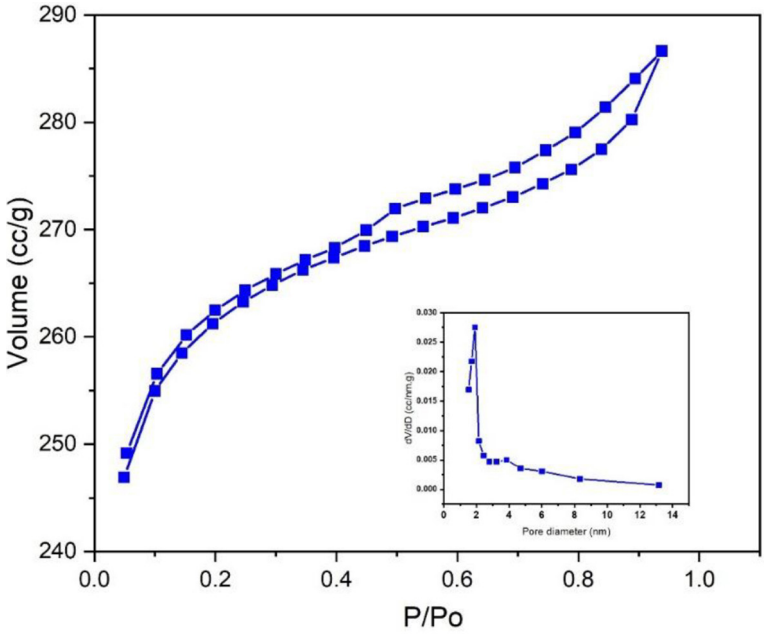

Figure 1. N_2 physisorption isotherms of fibrous carbon from acacia leaf. The inset indicates NLDFT PS distribution

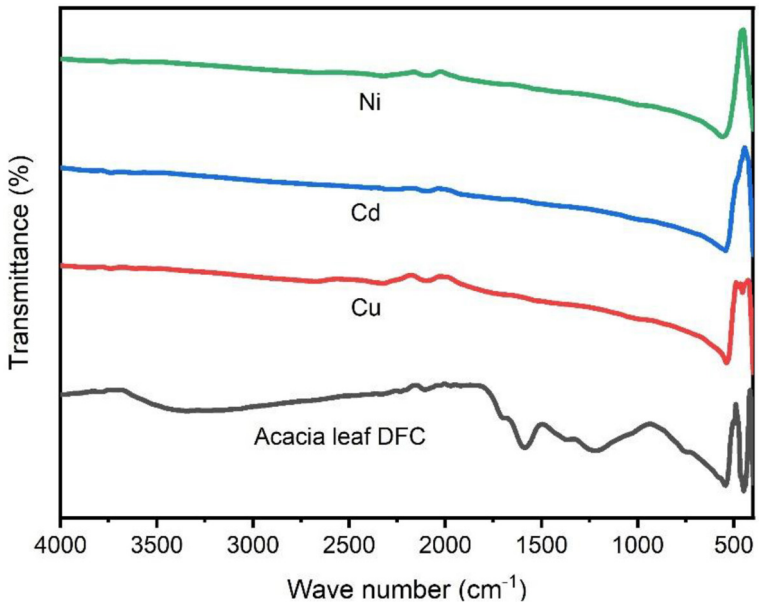

Figure 2. FTIR spectra of acacia leaf fibrous carbons before and after HM adsorption

Biosorbents comprise complex inorganic and organic materials like lipids, carbohydrate polymers, proteins, and sometimes metals (Sabzehmeidani et al., 2021; Pandey et al., 2024). Adsorption processes like ion exchange and chemisorption depend highly on the functional groups available in biosorbents (Raji et al., 2023). Generally, carbon and carbon-oxygen bonds attract and accelerate metal adsorption. From the FTIR analysis of acacia leaf fibrous carbons, there are several functional groups such as O–H stretch for carboxylic acids and N–H groups (between 3700 and 2500 1/cm). The wave number range of 1550-1640 1/cm shows C=C bands and the asymmetric stretching of the $–COO^-$ group. Wave numbers of 1320 and 1000 1/cm show the O–H stretch for alcohols/carboxylic acids (Pavia, 2001). These functional groups adsorb HM because of their capacity to create complex compounds. Changes in the FTIR spectra occur

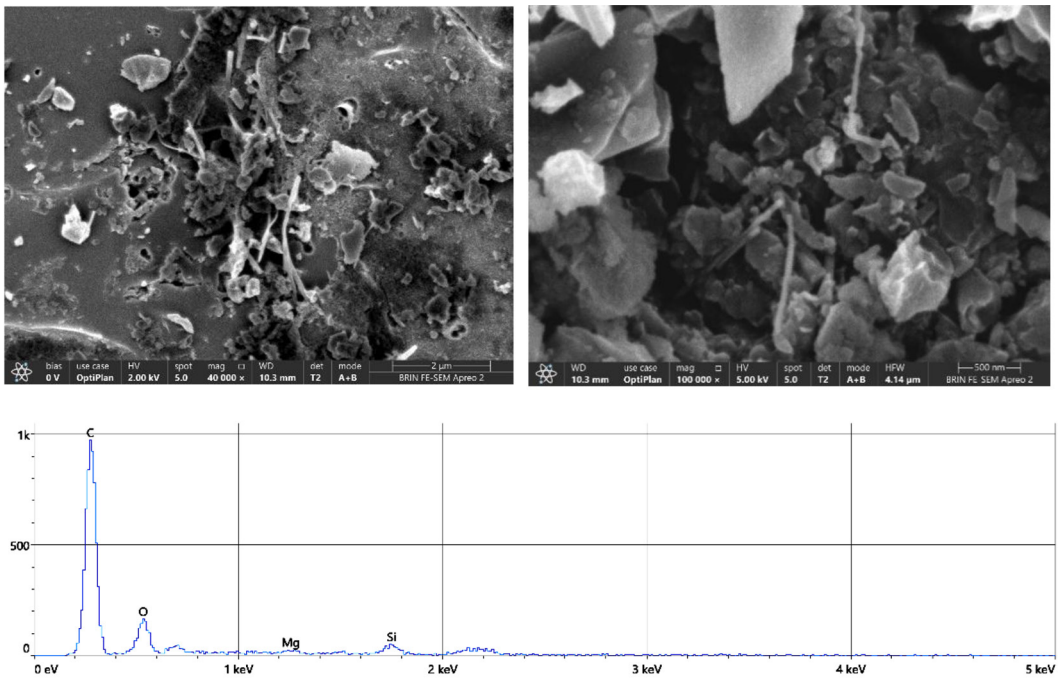

Figure 3. SEM photographs and EDS spectra of adsorbents

following the Cu(II), Cd(II), and Ni(II) adsorption. All metals exhibit a higher stretching peak (about 3740 1/cm). This shift represents the OH groups interaction with metal ions, which alters the bonding environment and vibration frequency. The signal at 1218.93 1/cm associated with C-O and C=O groups decreased following adsorption, indicating that functional groups with oxygen operate as active sites in binding metal ions. The decrease encourages surface complexation and ion exchange, where metal ions form coordination bonds or exchange places with H^+ attached to functional groups (Ye et al., 2022; Simamora et al., 2024).

SEM analysis

The adsorbent's chemical composition and morphology were analyzed using EDS and FE-SEM. FESEM analysis (Figure 3) revealed a distinct fibrous morphology with fiber diameters from 58–118 nm. These results are in line with the architecture of acacia-based carbon standards (Apriwandi et al., 2020). This unique structural configuration provides a large mesopore network (0.405 cm^3/g) that ensures the availability of abundant micropore binding sites. The carbonization procedure and chemical activation at high temperatures facilitated the lignocellulosic components etching, such as lignin, cellulose, and hemicellulose. These components have contributed to the nanostructure formation, which contains oxygen, silica, and carbon. EDS confirmed high purity with carbon (71.4%) and oxygen (20.1%) as the primary constituents.

Adsorption kinetics

Kinetics is needed to understand adsorption rates and identify rate-limiting steps. Sorption rate constants and reaction orders are crucial physicochemical parameters for evaluating the quality of an adsorbent. The kinetic models employed include PFO, PSO, Elovich, and intra-particle diffusion models. In the PFO model, physisorption governs the adsorption process, whereas in the PSO model, chemisorption is considered the rate-limiting step. The Elovich kinetic model is particularly useful for representing adsorption on heterogeneous surfaces, where the adsorption

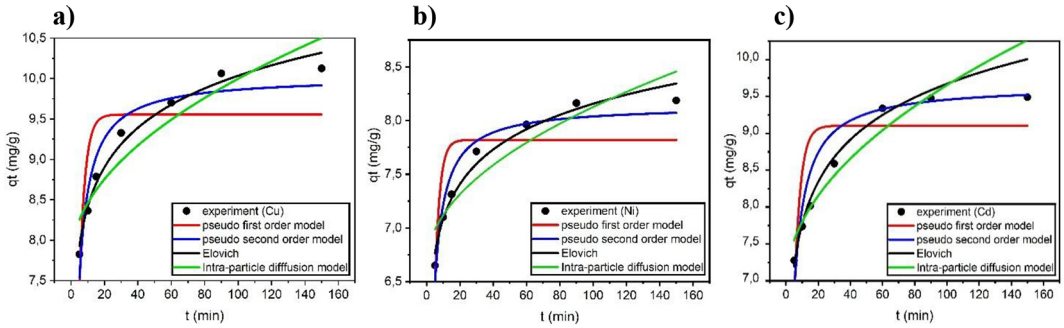

Figure 4. Adsorption kinetics: (a) Cu(II), (b) Ni(II), (c) Cd(II)

Table 2. Kinetic model parameters of Cu(II), Ni(II), and Cd(II) adsorption

Parameters		Cu(II)	Ni(II)	Cd(II)
PFO	R^2	0.618	0.622	0.517
	AICc	-2.636	-8.442	1.214
	k1 (min^{-1})	0.298	0.347	0.266
	qe (mg/g)	9.554	7.819	9.104
PSO	R^2	0.929	0.942	0.856
	AICc	-14.467	-21.581	-7.243
	k2 (mg/g.min)	0.060	0.096	0.049
	qe (mg/g)	10.025	8.140	9.654
Elovich	R^2	0.981	0.972	0.986
	AICc	-23.555	-26.553	-23.634
	α (mg/g.min)	11119.66	193897.46	1006.71
	β (g/mg)	1.422	2.151	1.211
Intra-particle diffusion (linear)	R^2	0.999	0.984	0.995
	K_{id1}	0.588	0.409	0.453
	C_1	6.509	5.758	6.275

activation energy increases exponentially with surface coverage. Meanwhile, the intra-particle diffusion model accounts for the adsorbate molecules movement from the solution to the pores. Figure 4 shows the nonlinear fitting curves of the kinetic models used, while the kinetic parameters are tabulated in Table 2.

To determine the most precise model for this process, we employed not only the coefficient of determination (R^2), which is frequently biased towards models with more parameters. Instead, we also used the AICc, which can balance the model fit and complexity by penalizing models that tend to overfit simply because they have more variables. Statistically, the model with the lowest AICc is considered superior because it minimizes the loss of information.

Furthermore, Table 4 describes the Elovich model consistently becomes the best model for the three metals. This is indicated by the lowest AICc value. The significant difference in AICc values between the Elovich and PSO models provides strong statistical justification for selecting the Elovich model. It shows the adsorption mechanism tends to be a chemisorption process on a heterogeneous surface (Peers, 1965). This is reinforced by the Elovich kinetic constant (β), which reflects a decrease in activation energy as the density of adsorbate on the surface increases. This also confirms the existence of binding sites with varying energy levels on acacia leaf fibrous carbon.

The rate-limiting processes are further investigated using intraparticle diffusion studies. The intra-particle diffusion stage has three distinct linear segments (Figure 5). External film diffusion is the first step, where metal ions rapidly diffuse from the solution to the outer surface (film diffusion). This is characterized by a steep segment. The decrease in the rate constant value at this stage indicates that diffusion into the pore structure is a significant rate-limiting factor. The third stage, which is nearly horizontal in length, shows that adsorption slows considerably after equilibrium is reached, as the active sites within the pores become saturated. Figure 7 shows a non-zero intercept ($C > 0$), indicating the presence of boundary layer resistance in mass transfer in addition to intraparticle diffusion. The presence of these several stages reveals that mass diffusion and surface chemical interactions govern the adsorption process overall rate (Xiong et al., 2018). The analysis focuses on the importance of microporous and mesoporous structures, as revealed by BET analysis, in enhancing adsorption. Micropores provide abundant binding sites, while mesopores enable efficient diffusion of metal ions into the adsorbent.

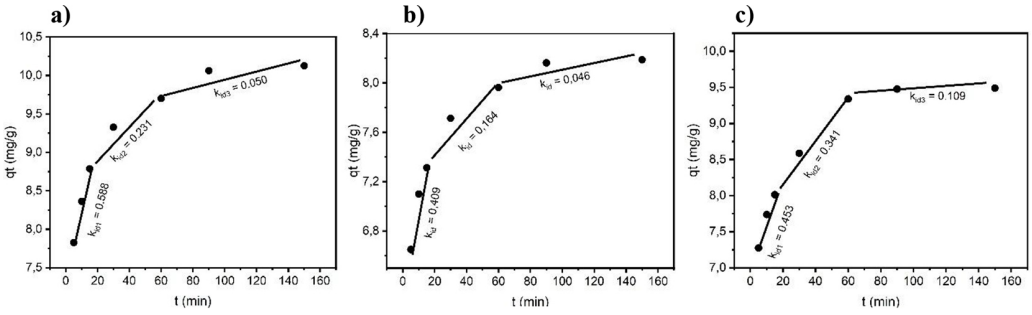

Figure 5. Linear regression applying the intra-particle diffusion model of (a) Cu(II), (b) Ni(II), (c) Cd(II)

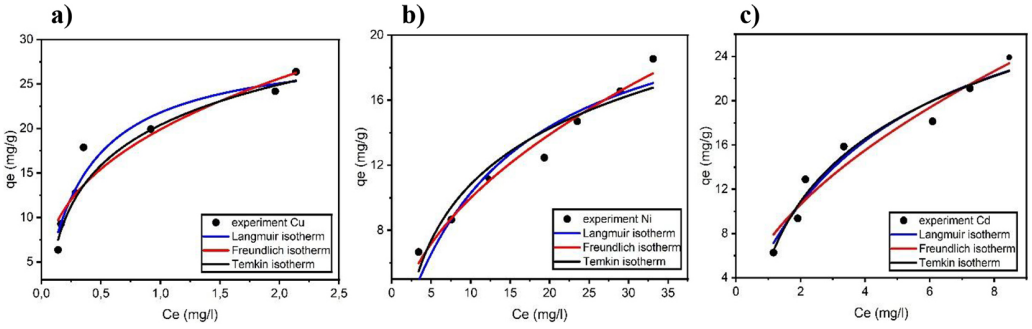

Figure 6. Adsorption isotherm models of (a) Cu(II), (b) Ni(II), (c) Cd(II)

Table 3. Adsorption isotherm parameters of Cu(II), Ni(II), Cd(II) adsorption on acacia leaf fibrous carbon in a single metal system

Parameters		Cu(II)	Ni(II)	Cd(II)
Langmuir	R^2	0.948	0.919	0.956
	AICc	12.457	-7.213	9.856
	qm (mg/g)	29.53	23.83	34.83
	K_L (L/g)	2.816	0.076	0.222
	R_L	0.004–0.018	0.127–0.363	0.050–0.183
Freundlich	R^2	0.904	0.974	0.947
	AICc	17.732	0.673	11.057
	K_F (mg/g)(L/mg)$^{1/n}$	19.89	3.33	7.28
	n	2.739	2.100	1.830
Temkin	R^2	0.985	0.920	0.965
	AICc	32.963	8.434	8.719
	A_T (L/mg)	22.32	0.883	1.889
	b (J/mol)	6.567	4.967	8.182

Table 4. Langmuir isotherm parameters of Cd(II), Ni(II), as well as Cu(II) adsorption on acacia leaf fibrous carbon in the two-metal system

Cd(II) – Cu(II)	Cu(II) – Ni(II)	Cd(II) – Ni(II)
For Cd(II)	For Cu(II)	For Cd(II)
$q_{m\text{-}Cd}$ = 6.12 (mg/g)	$q_{m\text{-}Cu}$ = 18.06 (mg/g)	$q_{m\text{-}Cd}$ = 10.93 (mg/g)
$K_{L\text{-}Cd}$ = 0.621 (L/g)	$K_{L\text{-}Cu}$ = 1.135 (L/g)	$K_{L\text{-}Cd}$ = 0.123 (L/g)
R^2 = 0.938	R^2 = 0.997	R^2 = 0.994
For Cu(II)	For Ni(II)	For Ni(II)
$q_{m\text{-}Cu}$ = 21.46 (mg/g)	$q_{m\text{-}Ni}$ = 16.87 (mg/g)	$q_{m\text{-}Ni}$ = 5.66 (mg/g)
$K_{L\text{-}Cu}$ = 1.189 (L/g)	$K_{L\text{-}Ni}$ = 0.032 (L/g)	$K_{L\text{-}Ni}$ = 0.078 (L/g)
R^2 = 0.968	R^2 = 0.921	R^2 = 0.973

Adsorption isotherms and favorability

Single metal adsorption

Isotherm analysis is useful for studying the adsorbate and adsorbent interaction under equilibrium conditions. The experimental data were observed applying the Langmuir, Freundlich, and Temkin isotherm models, with model selection based on the AICc for statistical rigor described in Figure 6 and Table 3.

The Langmuir model (lowest AICc) explained the uptake of Cu(II) and Ni(II), while the Temkin model provided the best fit for Cd(II) data, consistent with surface heterogeneity. The strong fit with the Temkin model indicates that the adsorption involves adsorption heat that decreases logarithmically with increasing surface coverage. These results are physically consistent with the heterogeneity of the acacia leaf fibrous carbon surface and are in line with the Elovich kinetic model. R_L values (0.004–0.363) confirm the process is highly favorable at 298K (Wen and Hu, 2021). Single-metal capacities followed the order Cd(II) (34.83 mg/g) > Cu(II) (29.53 mg/g) > Ni(II) (23.83 mg/g), controlled by the lower hydration free energy of Cd(II). In aqueous solutions, metal ions are surrounded by water molecules through a process called hydration. These ions must release some or all of the water molecules surrounding them (dehydration) in order to interact with the active sites. The dehydration process requires energy. Ions with higher hydration energy require more energy to undergo dehydration. Cu(II) and Ni(II) exhibit high hydration energies of -2100 and -2105 kJ/mol, respectively. In contrast, Cd(II) contains a lower hydration energy of -1807 kJ/mol, which facilitates its dehydration process. This can cause Cd(II) to more easily reach and occupy active sites, thereby resulting in the highest capacity in a non-competitive system (Liu et al., 2020).

Competitive adsorption

The Langmuir model selection for Cu(II) and Ni(II) metals in a single metal system, based on

Table 5. Langmuir extended isotherm parameters of Cu(II), Cd(II), as well as Ni(II) adsorption on acacia leaf fibrous carbon in the three-metal system

Cu(II) – Cd(II) – Ni(II)		
$q_{m\text{-}Cu}$ = 20.48 (mg/g) $K_{L\text{-}Cu}$ = 3.684 (L/g) R^2 = 0.941	$q_{m\text{-}Ni}$ = 6.15 (mg/g) $K_{L\text{-}Ni}$ = 0.188 (L/mg) R^2 = 0.979	$q_{m\text{-}Cd}$ = 16.02 (mg/g) $K_{L\text{-}Cd}$ = 0.050 (L/mg) R^2 = 0.977

strict statistical parameters (AICc), supports the extended Langmuir model application (Equation 9) for competitive modeling. The extended Langmuir model is a simplified version of the IAST (Ideal Adsorbed Solution Theory). The results obtained (Tables 4 and 5) indicate a consistently strong antagonistic interaction for both binary and ternary systems. The maximum equilibrium adsorption capacity (qm) of each metal decreases significantly in the competing metals. The drastic decrease in the maximum equilibrium capacity of Cd(II) by 82.43% from a single system to a Cu–Cd binary system confirms the strong competition between the metals for limited binding sites. Adsorption in multimetal systems produces strong antagonistic interactions, where the predicted qm values for all multimetal systems are smaller than for single systems.

Mechanism for competitive HM adsorption

The intrinsic structure of fibrous carbon and specific electronic interactions significantly influence the HM adsorption mechanism. The large SA (800,405 m²), hierarchical micro- and mesoporous structure, and the Elovich kinetic model, which is highly suitable for all three metals, indicate that the process occurring is chemisorption on a heterogeneous surface. Furthermore, the multi-segment Weber-Morris plot confirms that the rate-limiting steps for mass transfer are external film and intraparticle diffusion (Jie et al., 2017). The findings are also in line with the double pores that facilitate rapid access to active binding sites.

The maximum adsorption capacity shows the order Cd(II) > Cu(II) > Ni(II), with values of 34.83, 29.53, and 23.83 mg/g, respectively. The adsorption is more controlled by the hydration free energy. Cd(II), which has the lowest hydration energy (-1807 kJ/mol), undergoes dehydration more easily and can reach the active site faster than Cu(II) and Ni(II), which have higher hydration energies (-2100 and -2105 kJ/mol, respectively). Conversely, in a multimetal system, there is intense competition for active sites, so the control mechanism shifts to the formation of stable surface complexes. Under these conditions, Cu(II) shows absolute dominance with a selectivity order of Cu(II) > Cd(II) > Ni(II).

Cu(II)'s competitive advantage stems from its unique d^9 electronic configuration in an octahedral geometry. Based on the Jahn-Teller theorem, a non-linear system with an electronically degenerate ground state will be unstable and undergo spontaneous distortion to reduce its symmetry and energy (Halcrow, 2013). In the $[Cu(H_2O)_6]^{2+}$ complex, this distortion manifests as axial elongation, where the water molecule ligands on the z-axis move away from the metal center. Energetically, this elongation drastically reduces the overlap between the metal d orbitals and the axial ligands, causing in a significant decrease in energy in orbitals with z components, especially the d_z^2 orbital. This creates greater net energy stabilization for Cu(II) through ligand field stabilization energy (LFSE) when coordinating with oxygen functional groups (OH, COO), which are abundant on the ALFC surface (Fouad et al., 2021). In addition to its thermodynamic advantages, the Jahn-Teller distortion confers Cu(II) with exceptional kinetic lability (Charoensuk et al., 2021). The elongated, significantly weakened axial bonds lower the activation energy barrier for the ligand-exchange process. This allows Cu(II) to release part of its hydration shell and replace it with ligands on the adsorbent surface much faster than Ni(II) (d^8) (Liu et al., 2011). Although Ni(II) has a hydration radius nearly identical to Cu(II) (4.04 Å vs. 4.19 Å), the absence of Jahn-Teller distortion in Ni(II) makes its octahedral coordination more rigid or kinetically "inert." As a result, Ni(II) is less competitive in reaching and locking onto active sites than the more flexible Cu(II) (Neubrand et al., 2002).

The strong coordination bonds between the metal center and oxygenated ligands are marked by a shift in the C-O/C=O strain from 1218.93 1/cm. This shift indicates the presence of surface functional groups. Although Ni(II) possesses a smaller effective hydration radius (4.04 Å) than Cu(II) (4.19 Å), its inability to become unstable

Table 6. Maximum adsorption capacity of Cu(II), Ni(II), and Cd(II) on acacia leaf fibrous carbons with other adsorbents

Adsorbent	HM	Max sorption capacities (mg/g)	pH	Initial concentration (mg/L)	Reference
ALFC	Cd(II)	34.83	5	20-80	This study
Carbon nanotube		11.51	5.6	10-300	Akl and Elanwar, 2015
Cattle manure biochar		31.3	5.2	0.05-160	Wang et al., 2020
Sepiolite		22	5	10-100	Padilla-Ortega et al., 2011
Brewer's spent grain (BSG)		24.72	4.5	10-250	Dancker et al., 2025
Norway Spruce biomass		6.3	5-6	10-100	Al-Labadi et al., 2025
Pachira aquatica Aubl. fruit peel biochar		30.44	7.6	10-100	Nascimento et al., 2024
ALFC	Cu(II)	29.53	5	20-80	This study
Cattle manure biochar		14.7	5.2	0.05-160	Wang et al., 2020
Sepiolite		13.8	5	10-100	Padilla-Ortega et al., 2011
Norway Spruce biomass		7.9 mg/g	5-6	10-100	Al-Labadi et al., 2025
Spent mushroom substrate *Coprinus comatus*		19.09 mg/g	6	10-50	Yenie et al., 2025
ALFC	Ni(II)	23.86	5	20-80	This study
Multiwalled carbon nanotubes		6.09	7	5-100	Abdel-Ghani et al., 2015
Pachira aquatica Aubl. fruit peel biochar		5.65	7.6	10-100	Nascimento et al., 2024
Cattle manure biochar		11.1	5.2	0.05-160	Wang et al., 2020
Gamma-sterilized biowaste		23.88	5	25-500	Bambal et al., 2024

due to the Jahn-Teller effect prevents it from competing with Cu(II) in binding specific sites. Similarly, Cd(II) has a larger hydration radius (4.26 Å), which provides it with additional steric hindrance when competing with Cu(II) for accessing the microporous network of acacia leaf fibrous carbons.

Quantitative validation of Cu(II) adsorption on acacia leaf fiber carbon adsorbents can be performed using Density Functional Theory (DFT) calculations. A DFT study modeling the divalent metal ions interaction with oxygen-containing functional groups, which are considered to represent the dominant hydroxyl and carboxyl active groups found in biosorbents, produced the following absolute bond energy (E_ads) sequence: |E_ads(Cu)| > |E_ads(Ni)| > |E_ads(Cd)| (Ezzat et al., 2020). These results confirm that Cu(II) forms the most thermodynamically favorable bond, followed by Ni(II) and Cd(II) (Boulaiche, 2019). By linking macroscopic competitive behavior with this fundamental electronic structure, acacia leaf fibrous carbon has been proven to be efficient for selectively removing HM.

Comparison with other adsorbents

A adsorption capacities comparison of Cu(II), Ni(II), and Cd(II) on acacia leaf fibrous carbons with those of other adsorbents is presented in Table 6. The acacia leaf fibrous carbons' adsorption capacity is superior to that of other adsorbents. These superior adsorption capacities are attributed to the large SA (800.405 m^2/g), the presence of both micropores and mesopores, and a high oxygen functional groups concentration.

CONCLUSIONS

Kinetic analysis indicated that chemisorption on a heterogeneous surface governs the process, as described by the Elovich model selected based on AICc. In single-metal systems, adsorption selectivity followed the order Cd(II) > Cu(II) > Ni(II), primarily influenced by hydration free energy. In competitive multimetal systems, selectivity shifted to Cu(II) > Cd(II) > Ni(II), reflecting the dominant role of electronic coordination stability. The observed trend can be rationalized by ligand field stabilization and Jahn-Teller effects affecting Cu(II) kinetics. These findings provide a mechanistic basis for designing selective biomass-derived carbon adsorbents. The use of inexpensive, sustainable precursors aligns with circular economy principles. This study did not assess the spectroscopic validation of inner-sphere complexation (e.g., via

XPS), the durability and regeneration of the adsorbent through multi-cycle testing, performance in real industrial wastewater, or the techno-economic feasibility of KOH activation at scale, representing gaps that remain to be addressed for a comprehensive understanding.

Acknowledgments

The authors sincerely acknowledge the Research, Technology, and Community Service Directorate (DRTPM) as well as the Research and Community Service Institute (LPPM), University of Riau (Contract: 083/E5/PG.02.00.PL/2024 and 20636/UN.19.5.3.1/ AL.04/2024) for supporting this analysis.

REFERENCES

1. Abbas, Z., Ali, S., Rizwan, M., Zaheer, I. E., Malik, A., Riaz, M. A., Shahid, M. R., Rehman, M. Z. ur, Al-Wabel, M. I. (2018). A critical review of mechanisms involved in the adsorption of organic and inorganic contaminants through biochar. *Arabian Journal of Geosciences*, *11*(16). https://doi.org/10.1007/s12517-018-3790-1
2. Abdel-Ghani, N.T., El-Chagaby, G.A., Helal, F.S. (2015). Individual and competitive adsorption of phenol and nickel onto multiwalled carbon nanotubes. *Journal of Advanced Research, 6*(3), 405–415. https://doi.org/10.1016/j.jare.2014.06.001
3. Akl, M., Abou-Elanwar, A.M. (2015). Adsorption studies of Cd (II) from water by acid modified multiwalled carbon nanotubes. *J. Nanomed. Nanotechnol*. *6*(6). https://doi.org/10.4172/2157-7439.1000327
4. Alam, M. M., Hossain, M. A., Hossain, M. D., Johir, M. A., Hossen, J., Rahman, M. S., Zhou, J. L., Hasan, A. T., Karmakar, A. K., Ahmed, M. B. (2020). The potentiality of rice husk-derived activated carbon: from synthesis to application. *Processes*, *8*(2), 203. https://doi.org/10.3390/pr8020203
5. Al-Labadi I.G., Horváth, M., Alkilani, A.T., Al-Ma'abreh, A.M., Bashir, M.J.K., Keshta, B.E., Hanbali, G., Al-Zoubi, W., Abukhadra, M.R., Alqhtani, H.A., Eid, M.H. (2025). Simultaneous adsorptive removal of Pb2+, Cd2+, Cu2+, and Zn2+ using raw Norway Spruce biomass: a low-cost and eco-friendly solution for wastewater treatment. *Frontiers in Water*, *7*. doi.org/10.3389/frwa.2025.1612232
6. Amini, M., Rasat, M., Mohamed, M., Wahab, R., Ramle, N., Khalid, I., Yunus, AM. (2017). Chemical Composition of Small-Diameter Wild Acacia Mangium Species. *ARPN Journal of Engineering and Applied Sciences*, *12*(8), 2698–2702.
7. Apriwandi, Agustino, Erman T, Rika T. (2020). A high potential of biomass leaves waste for porous activated carbon nanofiber/nanosheet as electrode material of supercapacitor. *J. Phys.: Conf. Ser*. 1655, 012007. https://doi.org/10.1088/1742-6596/1655/1/012007
8. Ayach, J., Malti, W.E., Duma, L., Lalevee, J., Ajami, M.A., Hamad, H., H. A. (2024). Comparing Conventional and Advanced Approaches for Heavy Metal Removal in Wastewater Treatment: An In-Depth Review Emphasizing Filter-Based Strategies. *Polymers*, *16*, 1–25. https://doi.org/10.3390/polym16141959
9. Bambal, A., Jugade, R., Sarnavan, D., Pakade, Y. (2024). Sequestration of Ni(II) ions from water bodies by using gamma-sterilized biowaste. I*ndian Journal of Chemical Technology*. *31*, 738–748. doi.org/10.56042/ijct.v31i5.9238
10. Berber-Mendoza, M. S., Martínez-Costa, J. I., Leyva-Ramos, R., Amezquita García, H. J., Medellín Castillo, N. A. (2018). Competitive adsorption of heavy metals from aqueous solution onto oxidized activated carbon fiber. *Water, Air, and Soil Pollution*, *229*(8). https://doi.org/10.1007/s11270-018-3906-y
11. Bharti, S. (2024). Recent advances in heavy metal removal from wastewater using nanomaterials and cloud point extraction: a comprehensive review. *International Journal of Environmental Science and Technology*, *22*, 5057–5084. https://doi.org/10.1007/s13762-024-06068-8
12. Boulaiche, W. (2019). Kinetic and equilibrium studies of biosorption of M(II) (M = Cu, Pb, Ni, Zn, and Cd) onto seaweed Posidonia oceanica fibers. *Applied Water Science*, 9, 173. https://doi.org/10.1007/S13201-019-1062-1
13. Charoensuk, S., Tan, J., Sain, M., Manuspiya, H. (2021). A single crystal hybrid ligand framework of Copper(II) with stable intrinsic blue-light luminescence in aqueous solution. *Nanomaterials (Basel, Switzerland)*, *11*(9), 2281. https://doi.org/10.3390/nano11092281
14. Chen, X., Hossain, M. F., Duan, C., Lu, J., Tsang, Y. F., Islam, M. S., Zhou, Y. (2022). Isotherm models for adsorption of heavy metals from water - A review. *Chemosphere*, *307*, 135545. https://doi.org/10.1016/j.chemosphere.2022.135545
15. Ciobanu, R., Bucatariu, F., Mihai, M., Teodosiu, C. (2024). Silica-Based composite sorbents for heavy metal ions removal from aqueous solutions. *Polymers*, *16*(21). https://doi.org/10.3390/polym16213048
16. Danat, B.T., Wuana, R.A., Chahul, H.F. *et al.* (2026). Review of adsorption isotherms models. *Appl Water Sci 16*, 72. https://doi.org/10.1007/s13201-025-02682-0
17. Dancker, P., Brunner, D., Glas, K., Dawid, C., Gastl, M. (2025). Heavy metal adsorption of brewers spent grain in aqueous solution: Impact of mechanochemical esterification. *Brewing Science*, *78*, 47–54.

https://doi.org/10.23763/BrSc25-06

18. Darmayanti, L., Fitria, D., Edward HS., Yenie, E., Mayrizki, M., Winih, E.S. (2023). Hollow carbon fiber from waste biomass of acacia leaves for Fe (II) removal from aqueous solution. *Biomass Conversion and Biorefinery*, *14*, 23561–23590. https://doi.org/10.1007/s13399-023-04834-1
19. Das, T. K., Poater, A. Review on the use of heavy metal deposits from water treatment waste towards catalytic chemical syntheses. *International Journal of Molecular Sciences*, *22*(24), 13383. 2021. https://doi.org/10.3390/ijms222413383
20. Ezzat, H., Menazea, A.A., Omara, W., Basyouni, O.H., Helmy, S.A., Mohamed, A.A., Tawfik, W., Ibrahim, M. (2020). DFT: B3LYP/ LANL2DZ study for the removal of Fe, Ni, Cu, As, Cd, and Pb with chitosan. *Biointerface Research in Applied Chemistry*, *10*, 6, 7002–7010. https://doi.org/10.33263/BRIAC106.70027010
21. Ferraz, D., & Pyka, A. (2023). Circular economy, bioeconomy, and sustainable development goals: a systematic literature review. *Environmental Science and Pollution Research*. https://doi.org/10.1007/s11356-023-29632-0
22. Fouad, R., Shaaban, I. A., Ali, T. E., Assiri, M. A., Shenouda, S. S. (2021). Co(ii), Ni(II), Cu(II), and Cd(II)-thiocarbonohydrazone complexes: spectroscopic, DFT, thermal, and electrical conductivity studies. *RSC advances*, *11*(60), 37726–37743. https://doi.org/10.1039/d1ra06902k
23. Guo, Y., Yang, S. (2016). Heavy metal enrichments in the Changjiang (Yangtze River) catchment and on the inner shelf of the East China Sea over the last 150 years. *Science of the Total Environment*, *543*, 105–115. https://doi.org/10.1016/j.scitotenv.2015.11.012
24. Halcrow, MA (2013) Jahn-Teller distortions in transition metal compounds, and their importance in functional molecular and inorganic materials. Chemical Society Reviews, *42*(4). 1784–1795. http://dx.doi.org/10.1039/c2cs35253b
25. Jorge, A.O.S., Chamorro, F., Carpena, M., Barciela, P., Pérez-Vázquez, A., Oliveira, M. B. P. P. and Prieto, M. A. (2024). Recent Developments in the Removal of Heavy Metals from Water and Wastewater. *Proceedings*, *105*, 122. https://doi.org/10.3390/proceedings2024105122
26. Karthikeyan, S., Balasubramanian, R., Iyer, C. S. P. (2007). Evaluation of the marine algae Ulva fasciata and Sargassum sp. for the biosorption of Cu(II) from aqueous solutions. *Bioresource Technology*, *98*(2), 452–455. https://doi.org/10.1016/j.biortech.2006.01.010
27. Keshavarz, S., Okoro, O.V., Hamidi, M., Derakhshankhah, H., Azizi, M., Nabavi, S.M., Gholizadeh, S., Amini, S.M., Shavandi, A., Luque, R., Samadian, H. (2022). Synthesis, surface modifications, and biomedical applications of carbon nanofibers: Electrospun vs vapor-grown carbon nanofibers, *Coordination Chemistry Reviews*, *472*, 214770. https://doi.org/10.1016/j.ccr.2022.214770
28. Kim, J., Heo, Y.J., Hong, J.Y., Kim, S.K. (2020). Preparation of porous carbon nanofibers with tailored porosity for electrochemical capacitor electrodes. *Materials (Basel)*, *13*(3), 729. https://doi.org/10.3390/ma13030729
29. Kra, D.O., Allou, N.B., Atheba, P., Drogui, P., Trokourey, A.(2019). *Journal of Encapsulation and Adsorption Sciences*, *9*(2), 63–82, https://doi.org/10.4236/jeas.2019.92004.
30. Laus, R., De Fávere, V. T. (2011). Competitive adsorption of Cu(II) and Cd(II) ions by chitosan crosslinked with epichlorohydrin-triphosphate. *Bioresource Technology*, *102*(19), 8769–8776. https://doi.org/10.1016/j.biortech.2011.07.057
31. Li, Y., Gao, L., Lu, Z., Wang, Y., Wang, Y., Wan, S. (2020). Enhanced removal of heavy metals from water by hydrous ferric oxide-modified biochar. *ACS Omega*, *5*, 28702−28711.
32. Liu, J., YAO, P., NI, Z-M., LI, Yuan., SHI, Wei. (2011). Jahn-Teller effect of Cu-Mg-Al layered double hydroxides. *Acta Physico-Chimica Sinica*. *27*(9). https://doi.org/10.15244/pjoes/104455
33. Liu, X., Xu, X., Dong, X., Park, J. (2020). Competitive adsorption of heavy metal ions from aqueous solutions onto activated carbon and agricultural waste materials. *Polish Journal of Environmental Studies*, *29*(1), 749–761. https://doi.org/10.15244/pjoes/104455
34. Moustakas, K., Loizidou, M. (2024). Sustainable waste management and circular economy. *Environmental Science and Pollution Research*, *31*(12), 17525–17526. https://doi.org/10.1007/s11356-024-32347-5
35. Nascimento, T.L.S., Oliveira, K.F.S., Júnior, J.O.D., Pimenta, A.S., Melo, D.M.A., Melo, M.A.F., Braga, R.M. (2024). Biosorption of nickel and cadmium using *Pachira aquatica* Aubl. peel biochar. *Scientific Reports. 14*, 5086 (2024). https://doi.org/10.1038/s41598-024-54442-w
36. Neubrand, A., Thaler, F., Körner, M., Zahl, A., Hubbard, C.D., Eldik, R. (2002). Mechanism of water exchange on five-coordinate copper(II) complexes. *J. Chem. Soc., Dalton Trans.* 957–961. doi.org/10.1039/B107458J
37. Padilla-Ortega E, Leyva-Ramos R, Mendoza-Barron J, Guerrero-Coronado RM, Jacobo-Azuara A, Aragón-Piña A. (2011). Adsorption of heavy metal ions from aqueous solution onto sepiolite. *Adsorption Science & Technology*, *29*(6), 569-584. https://doi.org/10.1260/0263-6174.29.6.569
38. Pandey, K., Saharan, B.S., Kumar, R., Jabborova, D., Duhan, J.S. (2024). Modern-day green strategies for the removal of chromium from wastewater. *Journal of Xenobiotics, 14*(4), 1670–1696. https://doi.org/10.3390/jox14040089

39. Pavia DL, Lampman GM, and Kriz, GS. (2001). *Introduction to Spectroscopy.* Thomson Learning Inc., Third Edition.
40. Peers, A.M. (1965). Elovich adsorption kinetics and the heterogeneous surface. *Journal of Catalysis 4*, 499–503. https://doi.org/10.1016/0021-9517(65)90054-0
41. Pinto, F. R., Marcellos, C. F. C., Manske, C., Gomes Barreto, A., Jr (2024). Statistical analysis of parameters and adsorption isotherm models. *Environmental science and pollution research international*, *31*(41), 53729–53742. https://doi.org/10.1007/s11356-023-31820-x
42. Raji, Z., Karim, A., Karam, A., Khalloufi, S. (2023). Adsorption of heavy metals: mechanisms, kinetics, and applications of various adsorbents in wastewater remediation—a review. *Waste*, *1*(3), 775–805. https://doi.org/10.3390/waste1030046
43. Ruskova, K., Manoilova, L., Gonsalvesh-Musakova, L. (2025). Preparation and characterization of activated carbon based on acacia lignocellulosic biomass**.** *Journal of Chemical Technology and Metallurgy, 60*, 2, 287–292. https://doi.org/10.59957/jctm.v60.i2.2025.10
44. Sabzehmeidani, M.M., Mahnaee, S., Ghaedi, M., Heidari, H., Roy, V. A. L. (2021). Carbon-based materials: a review of adsorbents for inorganic and organic compounds. *Materials Advances 2*, 598–627. https://doi.org/10.1039/d0ma00087f
45. Shamim, S. (2018). Biosorption of Heavy Metals. https://doi.org/10.5772/intechopen 72099
46. Simamora, E., Nurcholis, M., Ardiani, A., Ernawati, R., Winarno, E. (2024). The potential of biochar for heavy metal adsorption in acid mine drainage based on literature review. *Journal of Earth and Marine Technology, 5*(1), 20–34. https://doi.org/10.31284/j.jemt.2024.v5i1.6772
47. Tan, P., Sun, J., Hu, Y., Fang, Z., Bi, Q., Chen, Y., Cheng, J. (2015). Adsorption of Cu2+, Cd2+, and Ni2+ from aqueous single metal solutions on graphene oxide membranes. *Journal of Hazardous Materials*, *297*, 251–260. https://doi.org/10.1016/j.jhazmat.2015.04.068
48. Vieira RH, Volesky B. (2000). Biosorption: a solution to pollution? *International Microbiology: the Official Journal of the Spanish Society for Microbiology*, *3*(1), 17–24. PMID: 10963329.
49. Wang, B., Lan, J., Bo, C., Gong, B., Ou, J. (2023). Adsorption of heavy metal onto biomass-derived activated carbon: review. *RSC Advances*, *13*, 4275–4302. https://doi.org/10.1039/d2ra07911a
50. Wang, X. S., Li, Z. Z. (2009). Competitive adsorption of nickel and copper ions from aqueous solution using nonliving biomass of the marine brown alga Laminaria japonica. *Clean-Soil, Air, Water*, *37*(8), 663–668. https://doi.org/10.1002/clen.200900045
51. Wang, S., Kwak, J. H., Islam, M. S., Naeth, M. A., Gamal El-Din, M., Chang, S. X. (2020). Biochar surface complexation and adsorption of Ni(II), Cu(II), and Cd(II) in aqueous solutions depend on feedstock type. *Science of the Total Environment*, *712*, 1–9. https://doi.org/10.1016/j.scitotenv.2020.136538
52. Wang, Y., Yan, X., Zhang, Y., Qin, X., Yu, X., Jiang, L., Li, B. (2024). Efficient removal of nickel from wastewater using copper sulfate–ammonia complex modified activated carbon: Adsorption Performance and Mechanism. *Molecules*, *29*, 2405. https://doi.org/10.3390/molecules29102405
53. Wen, J., Hu, X. (2021). Metal selectivity and effects of co-existing ions on the removal of Cd, Cu, Ni, and Cr by ZIF-8-EGCG nanoparticles. *Journal of Colloid and Interface Science*, *589*, 578–586. https://doi.org/10.1016/j.jcis.2021.01.021
54. Xiong, C., Wang, S., Zhang, L., Li, Y., Zhou, Y., Peng, J. (2018). Preparation of 2-aminothiazole-functionalized poly (glycidyl methacrylate) microspheres and their excellent gold ion adsorption properties. *Polymers*, *10*, 159. https://doi.org/10.3390/polym10020159
55. Ye, Q., Li, Q., Li, X. (2022). Removal of heavy metals from wastewater using biochars: adsorption and mechanisms. *Environmental Pollutants and Bioavailability*, *34*(1), 385–394. https://doi.org/10.1080/26395940.2022.2120542
56. Yenie, E., Darmayanti, L., Martina, A. Simarmata, S.D.P. (2025).The effect of temperature and adsorbate concentration on biosorption on Pb and Cu using spent mushroom substrate *Coprinus comatus*. *Int. J. Environ. Sci. Technology, 22*, 14137–14146). https://doi.org/10.1007/s13762-025-06547-6